Hydraulic Analysis of Harmonic Pumping Tests in Frequency and Time Domains for Identifying the Conduits Networks in a Karstic Aquifer

P Fischer, Abderrahim Jardani, M Cardiff, N. Lecoq, H Jourde

Research Paper/

Hydraulic Analysis of Harmonic Pumping Tests in Frequency and Time Domains for Identifying the Conduits Networks in a Karstic Aquifer

P. Fischer[1], A. Jardani[1], M. Cardiff[2], N. Lecoq[1], H. Jourde[3]

(1) Normandie Univ, UNIROUEN, UNICAEN, CNRS, M2C, 76000 Rouen, France

(2) Department of Geoscience, University of Wisconsin-Madison, Madison, WI, USA

(3) Hydrosciences Montpellier (HSM), Univ. Montpellier, CNRS, IRD, Montpellier, France

Conflict of interest: None

Corresponding author: P. Fischer

E-mail: pierre.fischer1@univ-rouen.fr

Key words: Oscillatory signal, Heterogeneity, Characterization, Aquifer, Frequency domain, Karst

Intended for publication in Journal of Hydrology

Abstract

In a karstic field, the flow paths are very complex as they globally follow the conduit network. The responses generated from an investigation in this type of aquifer can be spatially highly variable. Therefore, the aim of the investigation in this case is to define a degree of connectivity between points of the field, in order to understand these flow paths. Harmonic pumping tests represent a possible investigation method for characterizing the subsurface flow of groundwater. They have several advantages compared to a constant-rate pumping (more signal possibilities, ease of extracting the signal in the responses and possibility of closed loop investigation). We show in this work that interpreting the responses from a harmonic pumping test is very useful for delineating a degree of connectivity between measurement points. We have firstly studied the amplitude and phase offset of responses from a harmonic pumping test in a theoretical synthetic modeling case in order to define a qualitative interpretation method in the time and frequency domains. Three different type of responses have been separated: a conduit connectivity response, a matrix connectivity, and a dual connectivity (response of a point in the matrix, but close to a conduit). We have then applied this method to measured responses at a field research site. Our interpretation method permits a quick and easy reconstruction of the main flow paths, and the whole set of field responses appear to give a similar range of responses to those seen in the theoretical synthetic case.

1. Introduction

Characterization of the hydrodynamic properties of porous or fractured aquifers is a common challenge in many areas including: exploitation and protection of water resources, oil production, geothermal energy extraction, civil engineering, remediation engineering and storage of radioactive waste. Among many approaches (tracer tests, slug tests, geophysical investigations, etc.), this characterization can be accomplished using pumping tests, in which the values of the transmissivity and storativity parameters are derived from the analysis of the hydraulic responses to the aquifer stimulation (Butler 2005). However, in field conditions, many noise sources are unmanageable hydraulic contributions that can contaminate the signal induced by pumping, such as: aquifer recharge, river-aquifer interactions, evapotranspiration by plants, tidal fluctuations, or unplanned / unknown pumping at nearby water supply boreholes. For example, in unconfined aquifers evapotranspiration occurring during pumping tests may result in a spurious "signal" (see, e.g., Cardiff et al. 2009).

To address this difficulty, harmonic pumping tests have been suggested as an efficient approach to characterize the hydraulic properties, by making the hydraulic signal exploitable even for low signal amplitudes and noises corruptions (Cardiff and Barrash 2015). The oscillations in the hydraulic responses caused by a harmonic excitation with a known frequency can, in fact, be more easily extracted from the ambient noises, by applying filtering techniques (Bakhos et al. 2014), than the hydraulic responses generated by a constant rate pumping. Harmonic pumping tests also offer the possibility of avoiding the non-linear regimes of groundwater flow by controlling the characteristics of the periodic excitation. This excitation can be conducted through a pumping-reinjection system (Rasmussen et al. 2003), or even without any pumping or injection, by only using a moving mass (Guiltinan and Becker 2015). Harmonic pulse tests by using cyclic injection rates have also been conducted by Sun et al. (2015) and Sun et al. (2016) in a deep subsurface aquifer for leakage detection. Harmonic pumping tests have been

especially investigated for their abilities for characterizing aquifers properties. The analysis and interpretation of the harmonic data for a characterization are most often realized with analytical solutions (Renner and Messar 2006 ; Dagan and Rabinovich 2014 ; Rabinovich et al. 2015). Among these attempts, Black and Kipp (1981) proposed solutions for analytical models, under the homogeneity assumption, to derive the average transmissivity and storativity parameters from harmonic test analysis. Rasmussen et al. (2003) applied an analytical model expressed in frequency form to interpret the piezometric data generated from harmonic pumping tests in a porous contaminated aquifer, in order to estimate the average values of the hydraulic properties. The numerical models have also been used particularly in the frequency domain instead of the time domain in order to reduce the computing time and to take into account the spatial heterogeneity of the hydraulic properties (Black and Kipp 1981 ; Cardiff et al. 2013). Modeling and imaging potential of harmonic pumping tests data were also already addressed in the literature for the reconstruction of the spatial variability of hydraulic properties (Lavenue and de Marsily 2001; Cardiff et al. 2013; Zhou et al. 2016; Soueid Ahmed et al. 2016).

Some works have focused more specifically on the capacity of harmonic pumping for characterizing fractured aquifers. Renner and Messar (2006) applied harmonic pumping tests on a fractured sandstone aquifer to deduce the average values of transmissivity and storativity fields using a cyclical hydraulic excitation by alternating pumping, no flow and injection periods. At the same study site Maineult et al. (2008) used the self-potential method to monitor, remotely at the ground surface, the piezometric fluctuations caused by these harmonic excitations. More recently, Guiltinan and Becker (2015) similarly conducted periodic slug tests on isolated fractures without any extraction or injection, only by oscillating a slug at different depths of the water column in the well, to characterize the hydraulic connectivity of the fracture using analysis of phase shift and attenuation of the signal with an analytical model. Schuite et

al. (2017) used tilt data recorded at the ground surface to follow the oscillatory deformations induced by harmonic pulses performed in a fractured aquifer.

Among the works previously cited and dealing with this subject, none have sought to model the impact of spatial high contrasts of hydraulic property variations on oscillatory testing. In karstic aquifers, where low-transmissivity host rocks are directly adjacent to sparsely-distributed, high-transmissivity fractures and conduits, such a scenario is clearly present and leads to flow paths particularly constrained. Wells in karstic aquifers therefore may be expected to have drastically different responses depending on whether they are located on or near a fracture or a conduit. In fact, the main flow paths in subsurface karstic field follow the conduit and fracture network and one would need to have an idea of its positioning for understanding the flow behavior (White 2002 ; Saller et al. 2013). Commonly, karstic fields are described by their connectivity, whether the flows between wells follows a highly conductive path or not. Jazayeri et al. (2011) defined three types of hydrodynamic response to pumping and pulse tests, as a function of the degree of conductivity of the flow path network in the investigated karstic aquifer. The authors assumed that a short time lag and a high amplitude hydrodynamic response (conduit type hydrodynamic response) was the consequence of a high permeability and high connectivity between the observation well and the main flow path network (karst conduits that generate the large scale permeability of the aquifer), while ‘fracture type’ and ‘matrix type’ hydrodynamic responses were related to both a lower permeability and lower connectivity between the observation wells and the main flow path network. To be more consistent with previous works, this connectivity must be defined in term of property distribution as a ‘static’ or ‘topological’ connectivity, and in term of physical flow/transport processes as a ‘dynamical’ connectivity (Renard and Allard 2013; Tyukhova and Willmann 2016).

In this work, we propose an oscillatory signal analysis method, based on a synthetic and simplified model, for qualitatively interpreting hydraulic responses of a karstic field to a

harmonic pumping test performed at different frequencies. This method consists in interpreting the 'dynamical' connectivity information from the responses in terms of 'topological' connectivity within the karstic field. In the first section of the manuscript, we present the mathematical framework used to simulate numerically, in both temporal and frequency domains, the groundwater flow responses to a sinusoidal excitation in a fractured aquifer. These numerical approaches are applied in the second section to a hypothetical karstic aquifer characterized by the presence of a simple karstic network. In the third section, we perform signal analysis by comparing point measurements of spatial amplitude decay and phase shift values with respect to the source of the oscillating signal at the pumping well to determine a conduit (conduit network), dual (fissure, conduit proximity) or matrix flow connectivity. Finally, we apply the same analysis method on real field data acquired on a karstic field located in Southern France. This signal analysis method permits an easy, fast and coherent interpretation of the preferential flow paths' location on this site.

2. Theoretical background

In this article we use several terms such as harmonic, oscillatory, periodic, or sinusoidal signals, which all refer to the same idea of a signal defined by amplitude, a mean value and a period, repeating over time.

The harmonic pumping signal Q used in this manuscript is mathematically defined as:

$$Q(t) = -Q_A \cos(\omega t) + Q_m \ , \tag{1}$$

where t is the time (s), Q is the time-dependent flow rate signal (m^3/s), Q_A is the amplitude of the oscillatory portion of the flowrate signal (m^3/s), Q_m is the flow rate signal mean value (m^3/s), and $\omega = \frac{2\pi}{T}$ is the angular frequency where T denotes the period of the pumping signal

(s). We note that this flow formulation reproduces only the extraction of water with a flow rate sinusoidally fluctuating around the mean value Q_m. This flow rate signal can also be rewritten in a complex form:

$$Q(t) = -Q_{osc.}(t) + Q_m \ , \tag{2}$$

with $Q_{osc.}(t) = Re\left(Q_A e^{i\omega t}\right)$, and i representing the imaginary unit.

In order to describe the hydraulic drawdown responses of a confined karstic aquifer in 2D to a harmonic pumping signal, we represent the aquifer in a model domain Ω with a coupled discrete-continuum concept (for more details about the coupled discrete-continuum modeling, see Teutsch 1993 ; Liedl 2003). We combine Darcy's law and the law of conservation of mass in a 2D matrix domain (intact rock) containing a 1D discrete conduits domain, which gives us the following partial differential equations, both defined in the Cartesian coordinates dimension:

$$\begin{cases} S_{S,mat}\dfrac{\partial h}{\partial t} - \nabla\cdot\left(K_{mat}\nabla h\right) = \dfrac{-Q(t)}{V_{el.}}\delta\left(x - x_s\right) & \text{in the 2D matrix} \\ S_{S,cond}\dfrac{\partial h}{\partial t} - \nabla_T\cdot\left(K_{cond}\nabla_T h\right) = \dfrac{-Q(t)}{V_{el.}}\delta\left(x - x_s\right) & \text{in the 1D conduits} \end{cases} , \tag{3}$$

where h represents the hydraulic drawdown which links the 1D and the 2D domains (m), Q is the harmonic pumping rate (m^3/s) in an elementary volume V_{el} (m^3) of the matrix or the fractures, $\delta(x - x_s)$ represents the Dirac distribution where x_s denotes the coordinates of the pumping well that can be positioned in the matrix domain or in a conduit. $S_{S,mat}$ and $S_{S,cond}$ are the specific storages in the matrix and the conduits (m^{-1}), K_{mat} and K_{cond} are the conductivities in the matrix and the conduits (m/s), and ∇_T is the tangential gradient operator for the hydraulic equation in the conduits described as discrete elements at the internal boundaries of the domain.

Both governing equations can be solved numerically by following no-drawdowns initial and boundary conditions:

$$\begin{cases} h(x,y,t)=0 \quad \forall (x,y)\in \Omega \quad \text{when } t=0 \\ h(x,y,t)=0 \quad \forall t\geq 0 \qquad \text{when } (x,y)\in \Omega_{\text{boundary}} \end{cases} . \tag{4}$$

A sufficiently large equivalent porous media buffer zone encloses the model, in order to reduce the effects of the boundaries Ω_{boundary} on the flows within the model area of interest.

The nature of the excitation signal applied at the pumping borehole creates hydraulic responses $h(t)$ composed of a sinusoidal signature $h_{\text{osc.}}(t)$ and a non-sinusoidal signature $h_{\text{lin.}}(t)$, which must be eliminated to deal only with the harmonic component.

$$h(x,y,t)=h_{\text{osc.}}(x,y,t)+h_{\text{lin.}}(x,y,t) . \tag{5}$$

The hydraulic periodic signature $h_{\text{osc.}}$ can be expressed in a complex formulation:

$$h_{\text{osc.}}(x,y,t)=Re\left(H_{\omega}(x,y)e^{i\omega t}\right) . \tag{6}$$

where H_{ω} is a complex number representing the wave phasor at the given frequency.

Therefore we can compute numerically the harmonic responses due to the sinusoidal signal of the pumping rate by a reformulation of the time domain groundwater equation in a frequency domain (Black and Kipp 1981; Cardiff et al. 2013):

$$\begin{cases} i\omega S_{S,\text{mat}}H_{\omega}-\nabla\cdot\left(K_{\text{mat}}\nabla H_{\omega}\right)=\dfrac{Q_A}{V_{\text{el.}}}\delta(x-x_s) \quad \text{in the 2D matrix} \\ i\omega S_{S,\text{cond}}H_{\omega}-\nabla_T\cdot\left(K_{\text{cond}}\nabla_T H_{\omega}\right)=\dfrac{Q_A}{V_{\text{el.}}}\delta(x-x_s) \quad \text{in the 1D conduits} \end{cases} , \tag{7}$$

with H_{ω} the complex field variable which links the 1D and the 2D domains and describes the harmonic signal responses spatially.

153 In the frequency domain the initial and boundary conditions become:

154
$$\begin{cases} H_\omega(x,y) = 0 \quad \forall (x,y) \in \Omega \quad \text{initially} \\ H_\omega(x,y) = 0 \quad \text{when} \ (x,y) \in \Omega_{boundary} \end{cases} . \tag{8}$$

155 The amplitude and phase offset values of the response to the harmonic pumping signal at a
156 given position (x,y) are calculated from the complex variable H_ω value:

157 - *Amplitude*: $A(x,y) = \sqrt{\left(Re\, H_\omega(x,y)\right)^2 + \left(Im\, H_\omega(x,y)\right)^2}$ in m,

158 - *Phase offset*: $\Phi(x,y) = \frac{180}{\pi} atan2\left(-Im\, H_\omega(x,y), Re\, H_\omega(x,y)\right)$ in °, (9)

159 with *Re* the real part of H_ω, *Im* the imaginary part of H_ω, and *atan2* the two-arguments
160 inverse tangent function in radian mode (rad).

161 Then the time-dependent periodic response can be reconstructed as:

162
$$h_{osc.}(x,y,t) = A(x,y)\cos\left(\omega t - \Phi(x,y)\frac{\pi}{180}\right) . \tag{10}$$

163 Thus the frequency domain solver permits to reproduce periodic time-dependent responses
164 while avoiding the use of a time domain solver.

165 # 3. Synthetic application

166 ## 3.1.Model structure

167 In order to interpret drawdown responses to harmonic pumping tests in a real karstic aquifer
168 (Terrieu, Southern France), we have studied the spatial drawdown responses from a synthetic
169 case model of dimensions 50 m × 50 m. This synthetic case model was built in consideration of
170 our current understanding of the Terrieu karstic field (presented more specifically in section
171 4.1) and our pumping signals during investigations at the field site. A simple karstic network is

represented in the model as a 1D discrete geometry in a 2D continuum homogeneous matrix (Figure 1).

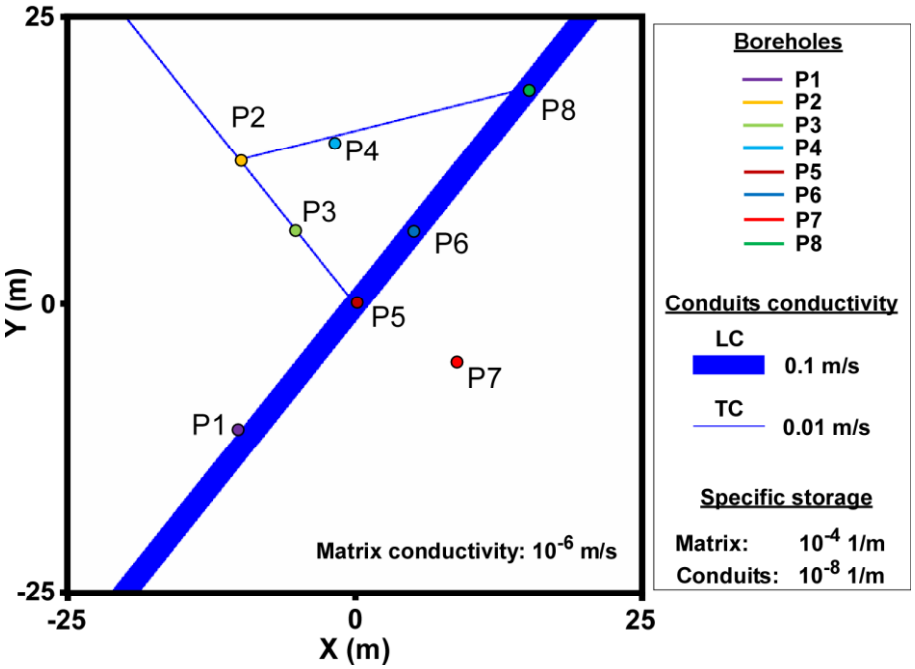

Figure 1: The theoretical synthetic case used to study the responses of a harmonic pumping in a karstic field. A karstic network (in blue) composed of a large conduit (LC) and two thin conduits (TC) crosses a homogeneous matrix (in white). All conduits are 1-D features in the model, but shown with conductivity-weighted thicknesses for clarity. Eight different boreholes are positioned in the model and represent pumping or measurement points.

The homogeneous matrix is associated with a 10^{-6} m/s conductivity value and a 10^{-4} m^{-1} specific storage value. The karstic network is composed of a large conduit with a 0.1 m/s equivalent hydraulic conductivity and two thin conduits with a 0.01 m/s equivalent hydraulic conductivity. The whole conduit network is associated with a 10^{-8} m^{-1} specific storage.

Eight different boreholes have been placed in this model at different strategic positions (Table 1). Three boreholes are located in the large conduit (LC: P5, P6, P8), two in the thin conduit (TC: P2, P3), two in the matrix but near to the conduit network (M-NC: P1, P4) and one in the matrix, distant from the conduit network (M: P7). We applied a 5 min period harmonic pumping signal (as defined in Eq. 1) in each of these boreholes alternatively, while measuring the

drawdown responses in the seven other boreholes. Different values of pumping amplitudes and mean flow rates were chosen according to the positioning of the pumping borehole (in a conduit or the matrix) in order to simulate a difference of productivity at each location.

Table 1: Coordinates, position and pumping signal parameters for the eight boreholes. For the positioning M=Matrix, TC=Thin Conduit, LC=Large Conduit and NC=Near Conduit. The pumping signal parameters are the amplitude (Q_A) and the mean flow rate (Q_m) (see Eq. 1).

	P1	**P2**	**P3**	**P4**	**P5**	**P6**	**P7**	**P8**
X ; Y (m)	-10 ; -11	-10 ; 12.5	-5 ; 6.25	-2 ; 14	0 ; 0	5 ; 6.25	9 ; -5	15 ; 18.75
Position	M-NC (1 m from LC)	TC	TC	M-NC (50 cm from TC)	LC	LC	M	LC
Q_A / Q_m (L/s)	0.5 / 1	2 / 4	2 / 4	0.5 / 1	2 / 4	2 / 4	0.5 / 1	2 / 4

The synthetic case model is enclosed in a 1,000 m × 1,000 m buffer zone with a global 10^{-3} m/s conductivity value and a 10^{-4} m^{-1} specific storage value. The boundaries of the buffer zone are associated with a no-drawdown condition. Thus the buffer zone reduces boundaries effects on drawdowns simulated within the central area of the model.

The governing equation (Eq. 3 and Eq. 7) for the simulation in the model were solved with the software COMSOL Multiphysics using a finite element method on a triangular adaptive grid (with a mesh refinement around the model discrete structures: the linear conduits and the boreholes points presented in Figure 1) considering the initial and boundary conditions described in Eq. 4 and Eq. 8.

3.2. Modeling in time domain

We firstly solved the synthetic case model in the time domain (Eq. 3). The top graphic in Figure 2 shows the time domain drawdown response in all boreholes for a harmonic pumping in P3 (in a thin conduit). Except for P7, we notice a periodic signal in the responses of each borehole. Moreover, past the first signal period, the drawdown responses can be represented as the sum of a linear drawdown (extracted by linear regression) and a purely oscillatory signal (Figure 2).

212 This oscillatory signal can be parameterized, for each borehole, by a value of amplitude and a
213 value of phase offset. In the particular case of P7, its oscillatory signal is almost null (< 1 mm),
214 thus its drawdown response is composed almost exclusively of a linear signal.

215

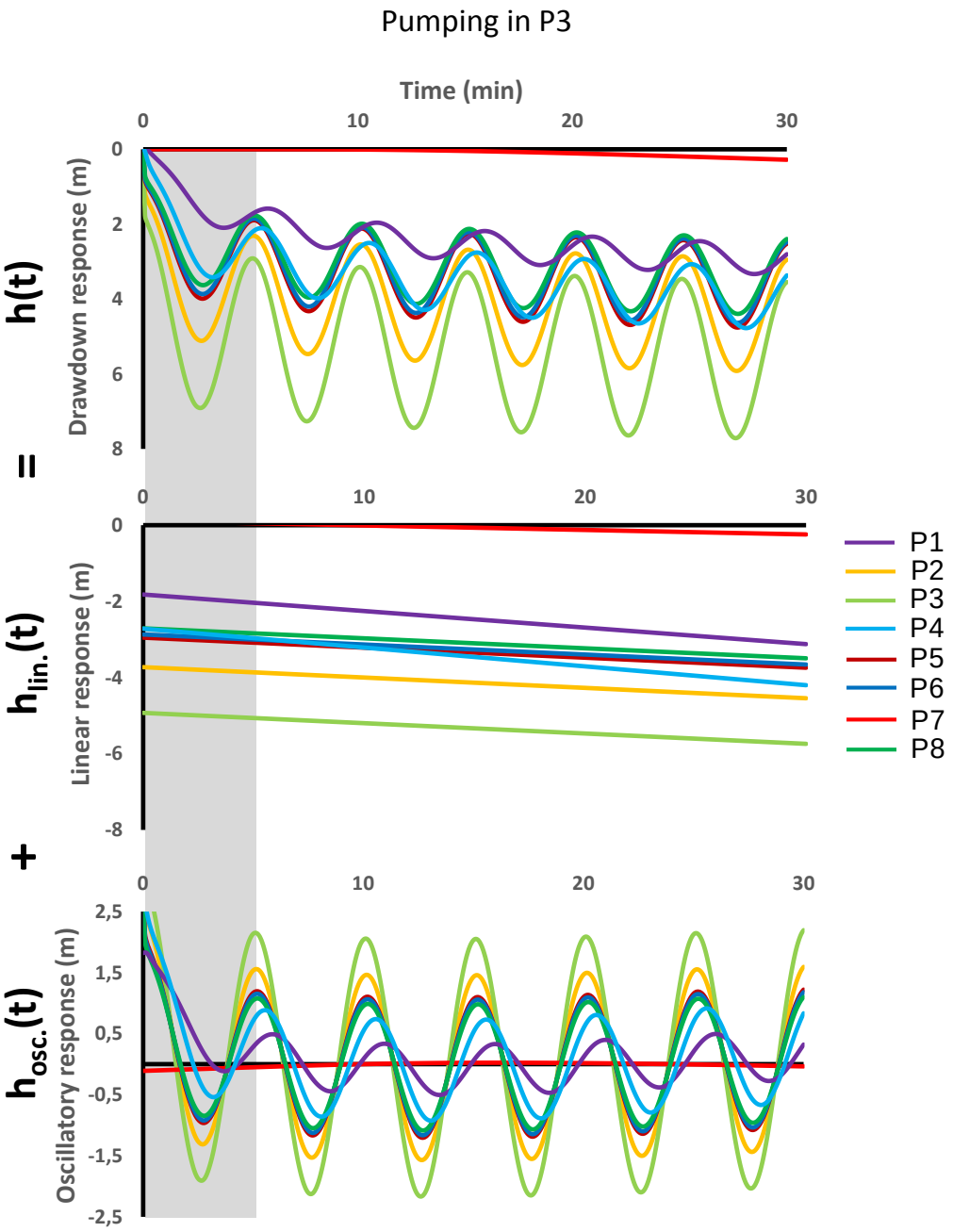

216

217 Figure 2: Drawdown responses h in each borehole to a harmonic pumping in P3 in a time
218 domain simulation. If the greyed portion of the time series is not considered, these drawdown

responses can be described as the sum of a linear signal $h_{lin.}$ and a purely oscillatory signal $h_{osc.}$.

From the observations made in Figure 2, the drawdown response at a given position, after the first signal period, can be mathematically approximated as the sum of a linear function and an oscillatory function:

$$h(t) \simeq \underbrace{-at - h_0}_{h_{lin.}(t)} + \underbrace{A\cos\left(\frac{2\pi}{T}t - \Phi\frac{\pi}{180}\right)}_{h_{osc.}(t)} + H_0 \ , \qquad (11)$$

with h (in m) the time domain drawdown response, $h_{lin.}$ (in m) the linear part of the response with its slope a (in m/min) and its intercept values h_0 (in m), $h_{osc.}$ (in m) the oscillatory part of the response with A (in m), Φ (in °) and T (in min) its amplitude, phase offset and period values, and H_0 (in m) the initial water level (in our synthetic case, this value is considered as 0).

For the interpretation of the responses we will be more specifically interested in the oscillatory response $h_{osc.}$.

3.3. Modeling in frequency domain

3.3.1. Frequency / Time domains comparison

We also solved the synthetic case in the frequency domain (Eq. 7). In this way, instead of spatial drawdown values, we calculate the spatial variation of amplitude and phase offset values in the response signal. We can then reconstruct for a given position the oscillatory signal $h_{osc.}$ in the drawdown response from these amplitude and phase offset values as described in Eq. 10. By comparing the reconstructed frequency domain signals to the time domain oscillatory ones, we show that they are almost identical (see the example for pumping in P3 in Figure 3 and

Appendix 1), except for the first signal period (see Figure 2), in which the time domain signals have not reached a stationary behavior (because of the pumping signal oscillating around a non-null mean rate).

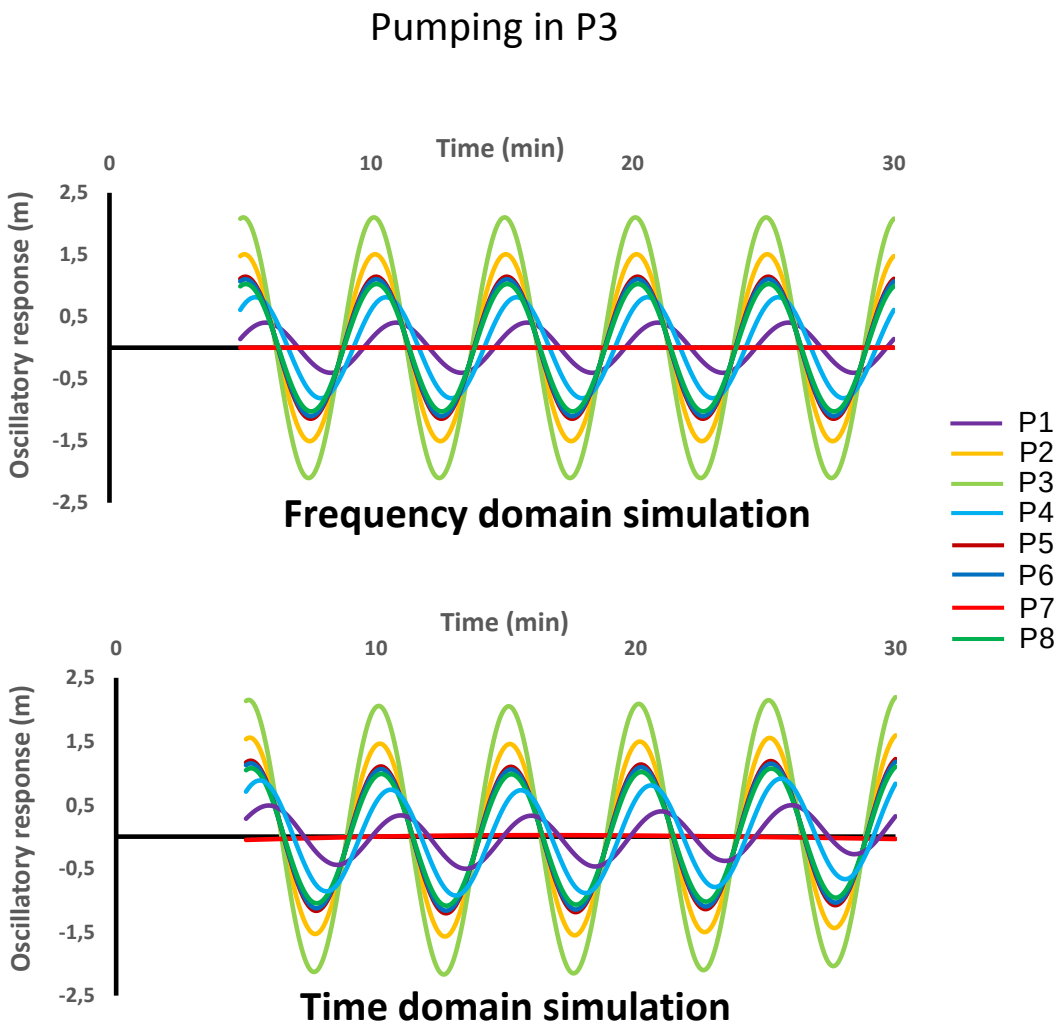

Figure 3: Oscillatory signals responses in each borehole for a harmonic pumping in P3, for a frequency domain simulation and a time domain simulation (avoiding the first signal period). One sees that these signals are almost the same for the two simulations.

We can simulate the same oscillatory responses signals to a harmonic pumping test either with a time domain solver, or with a frequency domain solver (if we put aside the first period where the time domain responses have not reach their stationary behavior, and thus are not

253 reproducible in the frequency domain). However, in our case, the frequency-domain solver is
254 more useful, as it provides directly the spatial distribution of the oscillatory responses amplitude
255 and phase offset values that interest us for the interpretation part. There is no need of signal
256 decomposition as in the time domain simulations. The frequency domain solver is also faster
257 than the time domain one as we don't have to simulate different time steps (for the simulations
258 on the presented synthetic case the frequency domain solver was approximately 120 times faster
259 than the time domain one).

260 Therefore, for the interpretation of the responses oscillatory signals $h_{osc.}$, we have used the
261 frequency domain simulations, and more specifically the responses' amplitude and phase offset
262 values at the position of the different boreholes.

263 3.3.2. Analysis of the harmonic hydraulic responses

264 In order to interpret the spatial responses to harmonic pumping at a point in the karstic synthetic
265 case, we have specifically studied the amplitude and phase offset values in these oscillatory
266 signal responses. We have observed that, depending on the pumping borehole location, the
267 responses could be highly variable. From Figure 4 we first state that the oscillatory signal
268 amplitude response is not proportional to the distance between the measurement points and the
269 pumping point, as it would be expected in a purely homogeneous aquifer. In our synthetic case,
270 the spatial responses were controlled by the degree of connectivity between the pumping point,
271 the flow path induced by the pumping, and the measurement point. In particular cases, if the
272 pumping borehole is positioned in the matrix, no oscillatory responses can be seen in the other
273 boreholes (see case P7 in Figure 4).

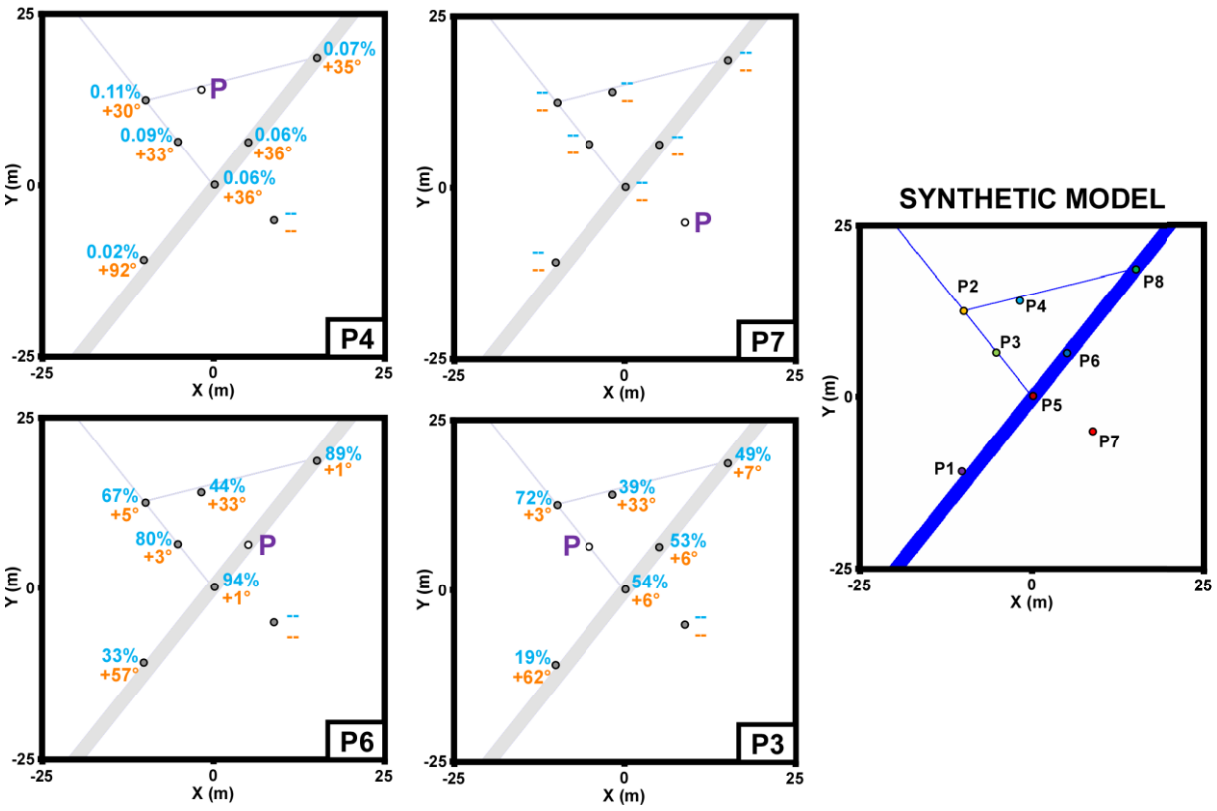

Figure 4: Relative amplitude (%, in blue) and relative phase offset (°, in orange) values in the oscillatory responses in each borehole for different harmonic pumping locations (P4, P7, P6, P3). A dash represents an absence of oscillatory response (< 1 mm). The pumping location is indicated by 'P' and its drawdown oscillatory signal is considered as a 100% amplitude signal with a 0° phase offset.

Four representative examples of response are presented in Figure 4, with the complete table of responses amplitudes and phases offsets for these cases presented in Appendix 2. From the analysis of the 8 different pumping cases in the synthetic model, if we pump in or near to a conduit, three degree of connectivity can be interpreted by comparing the spatial oscillatory responses relatively to the pumping signal:

- *Amplitude responses associated with a low phase shift* (see P2, P3, P5, P8 responses for a pumping in P3 or P6 in Figure 4): the pumping point is in a conduit and the measurement point has a *conduit connection* to it through a flow path in the karstic network,

- *Amplitude responses associated with a high phase shift*: the measurement point and the pumping point have a *dual connection*. A prevailing part of the flow path follows the karstic network and another part is in the matrix. The response phase offset value is proportional to the matrix flow path importance. Then, either the pumping point is in the matrix near to a karstic network (see P2, P3, P5, P8 responses for a pumping in P4 in Figure 4), or the measurement point is in the matrix near to the network (see P1 and P4 responses for a pumping in P3 or P6), or both with a higher phase offset (see P1 response for a pumping in P4),
- *Negligible amplitude responses (almost no oscillatory signal)* (see P7 responses in Figure 4): the prevailing part of the flow path between the measurement point and the pumping point is located in the matrix, it generates a *matrix connection* response.

Further information can be interpreted from the relative amplitude value of the measured signals for the responses with the same phase offset. If the flow path follows a thin conduit in the network, the amplitude of the signal will decrease along the flow path away from the pumping point (see the responses in the thin conduit for the pumping case P6). The rate of decay in the responses amplitude becomes less important when the signal reaches more conductive conduits of the network (see the amplitude decay of the responses in the large conduit for the pumping case P3). The decay rate is inversely proportional to the conductivity of the conduits.

The choice of the harmonic pumping period is important for a good interpretation of the oscillatory responses. We show, in Figure 5, the spatial responses' signal differences for harmonic pumping in P6 and P3 with a same signal amplitude (Q_A = 2 L/s) but two different periods (1min – 5min).

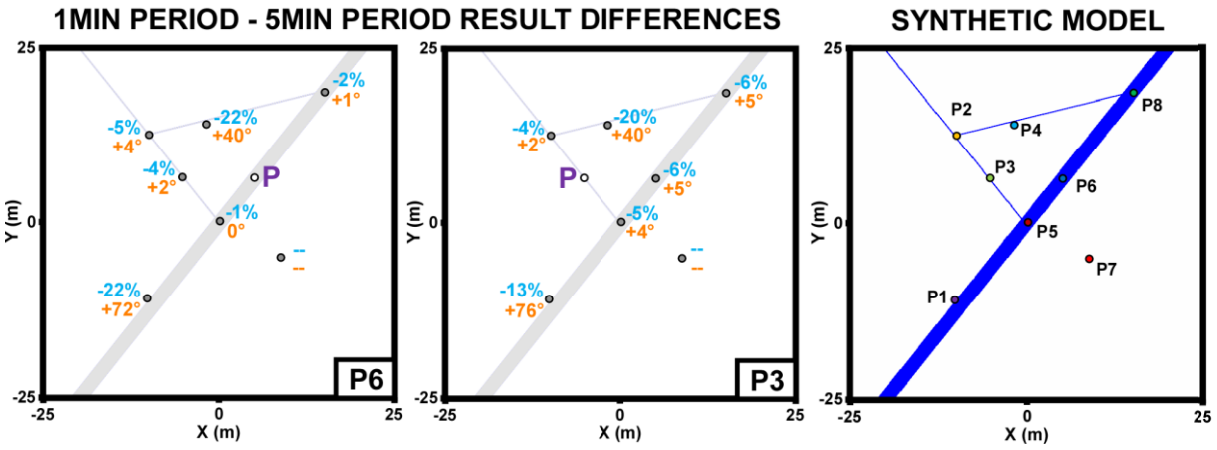

312

313 Figure 5: Differences in relative amplitude (in blue, in %) and relative phase offset (in orange,
314 in °) values in the oscillatory responses by decreasing from a 5 min period signal to a 1 min
315 period signal for two different harmonic pumping locations (P6, P3). A dash represents an
316 absence of oscillatory response (< 1 mm). The pumping location is indicated by 'P'. The main
317 signal differences appear for the boreholes located in the matrix, near to a conduit (P1, P4) (dual
318 connection).

319

320 The main effect of changing the period duration affects specifically the measurement boreholes
321 that have a dual connection to the pumping borehole, while the other boreholes will have little
322 consequent response differences. Decreasing the period from 5 min to 1 min will produce a
323 relative decrease of the amplitude and a relative phase offset increase in the response signal of
324 the boreholes with a dual conduit/matrix connection. Globally, this would tend to bring a 'dual
325 connectivity' response closer to a 'matrix connectivity' response. This can be clearly seen in
326 the oscillatory responses reconstructed from Eq. 10 (Figure 6). For a 1 min pumping period,
327 there is no significant signal changes for the boreholes in the conduits, but the oscillatory signals
328 for the boreholes in the matrix tend to disappear compared to their responses to a 5 min pumping
329 period signal (especially for P1 that becomes closer to the P7 'matrix connectivity' signal).

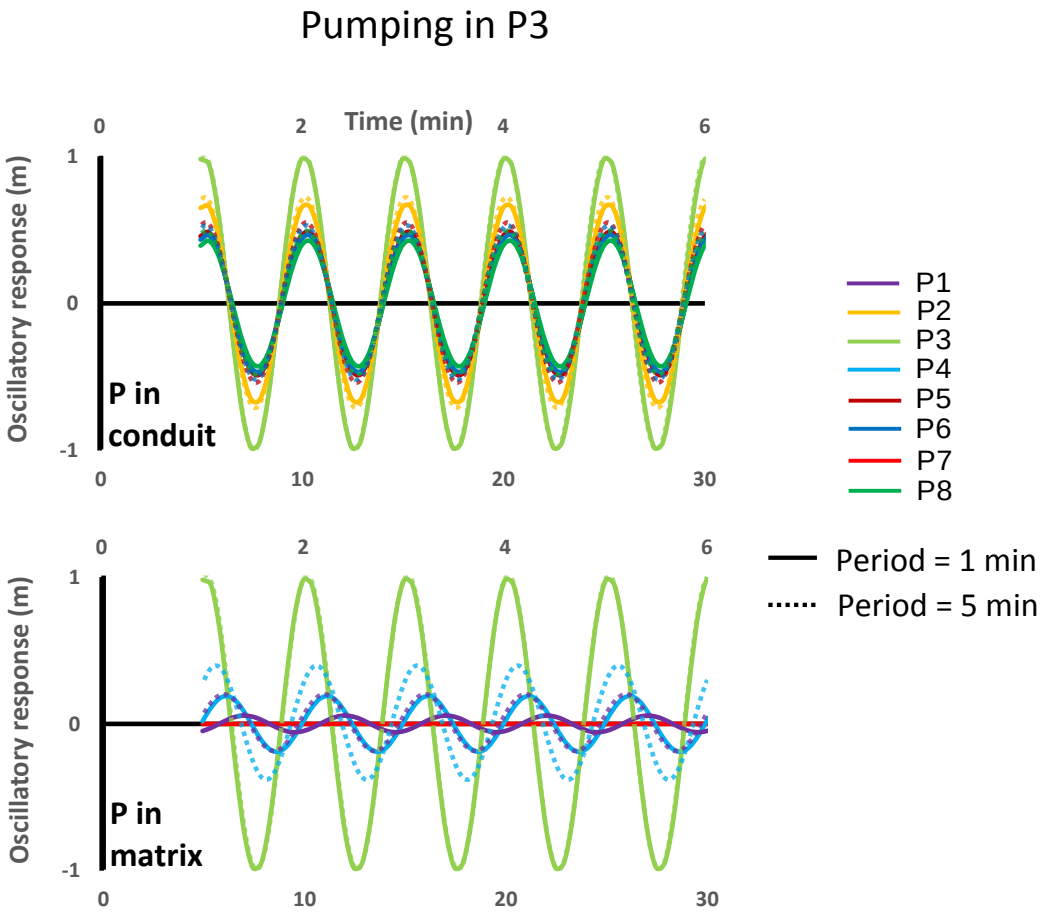

330

331 Figure 6: Comparison of the oscillatory relative responses for a harmonic pumping in P3 for a
332 1min period signal during 6 min (full line) and a 5min period signal during 30 min (dotted line).
333 The measurement boreholes have been separated regarding their location: in a conduit (P2, P5,
334 P6, P8) or in the matrix (P1, P4, P7). The main signal differences appear for the boreholes
335 located in the matrix, near to a conduit (P1, P4) (dual connection).

336

337 From the previous observation, we have studied the evolution of the relative amplitude and
338 phase offset responses more specifically in the points with a dual connection to the network
339 (P1, P4) for increasing periods (Table 2). It appears that the most important factor impacting
340 the responses in these points is their distances to the network. Independently from the
341 importance of the conduit in which the pumping is performed, the more a measurement point
342 is distant from the network the more its phase offset response will evolve with a period change
343 (see in Table 1 P1, distant from 1 m, compared to P4, distant from 50 cm). On the contrary, the
344 relative amplitude of the response seems to be related to the productivity of the pumping

location, but is therefore less interesting for delineating the position of the measurement point. Globally, for a good characterization of the conduits positioning, it is important to choose at least two different periods in order to compare the evolution of the phase offset in the responses. These periods should be sufficiently high to avoid the risks related to a too low amplitude response (unreadable response) or a phase offset value exceeding one cycle (see Table 2) that may lead to incorrect interpretations.

Table 2: Table of the relative amplitude and phase offset values in the oscillatory responses of P1 (1 m away from the network) and P4 (50 cm away from the network) to harmonic pumping in P3 and P6 and for increasing signal periods. In this table Amp.=Amplitude, P.O.=Phase Offset, TC=Thin Conduit, LC=Large Conduit, NTC=Near Thin Conduit and NLC=Near Large Conduit. Values in parentheses signify phase offsets greater than one cycle (>360°).

Pump. point	Meas. point		Period						
			10 s	30 s	1 min	2 min	5 min	10 min	30 min
P3 (TC)	P1 (NLC)	Amp.	2%	3%	6%	11%	19%	26%	37%
		P.O.	(-14°)	(+128°)	+138°	+96°	+62°	+45°	+27°
	P4 (NTC)	Amp.	4%	11%	19%	28%	39%	46%	55%
		P.O.	(+79°)	+107°	+73°	+52°	+33°	+24°	+16°
P6 (LC)	P1 (NLC)	Amp.	4%	6%	11%	19%	33%	44%	57%
		P.O.	(-20°)	(+124°)	+129°	+90°	+57°	+40°	+23°
	P4 (NTC)	Amp.	5%	13%	22%	32%	44%	53%	63%
		P.O.	(+51°)	+106°	+73°	+51°	+33°	+24°	+15°

To summarize, when pumping in the network, studying the amplitude of the responses provides some information about the conductivity of the conduits along the flow path, while studying the phase offset of the responses permits to characterize the degree of connectivity between the measurement points. A low period pumping (high frequency) tends to highlight more specifically the boreholes directly connected to the pumping point by conduits (network flow propagation). A high period pumping (low frequency) tends to generate responses in boreholes

with a conduit or a dual connectivity to the pumping point (part of network and part of diffusive flows propagation).

In order to locate only the boreholes directly connected through the conduit network, a high frequency pumping is necessary. But adding in combination responses from a lower frequency permits the identification of boreholes close to this network, which is useful information for imaging the karstic network arrangement.

3.3.3. Spatial analysis on simulation maps

The previous interpretation of the oscillatory signal responses to pumping signal with a 5 min period can be generalized in maps of spatial distribution of the amplitude (Figure 7) and phase offset (Figure 8) responses.

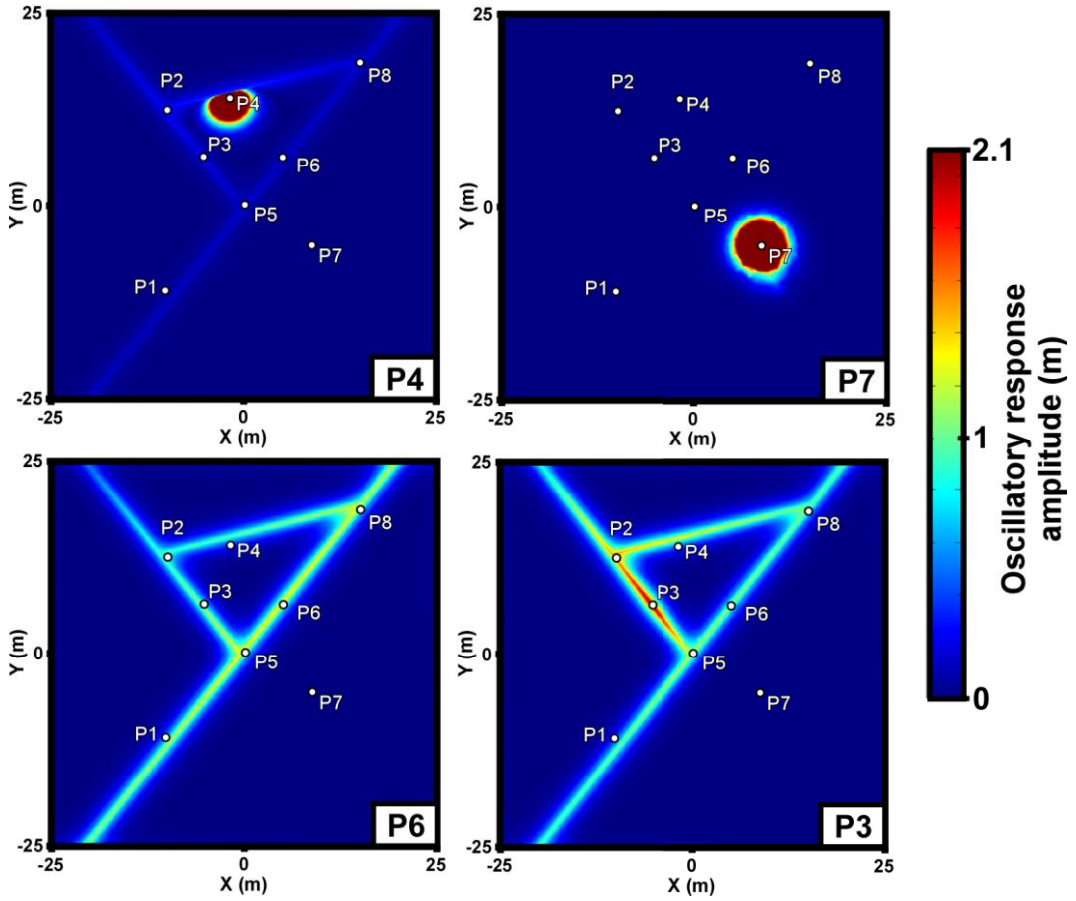

373

374 Figure 7: Maps of distribution of the amplitude value in the responses to a harmonic pumping
375 signal with a 5 min period at different locations: in the matrix near a conduit (P4), in the matrix
376 (P7), in a large conduit (P6), in a thin conduit (P3).

377

378 The case of a pumping in P7 (in the matrix) in Figure 7 shows a typical response map that would
379 be expected from a homogeneous aquifer with an amplitude response decreasing with the
380 distance to the pumping point forming a circle. In the case of a pumping in P4 (in the matrix),
381 this response circle reaches the karstic network and the signal can propagate in the conduits
382 with a subdued amplitude. If the pumping point is directly located in a conduit of the network
383 (P6 and P3), the oscillatory signal propagates uniquely through the flows of the conduits,
384 highlighting the karstic network. A linear decrease of the signal amplitude is visible in the thin
385 conduits along the flow path, but in the most conductive conduits, the signal easily propagates
386 at a site scale without attenuation.

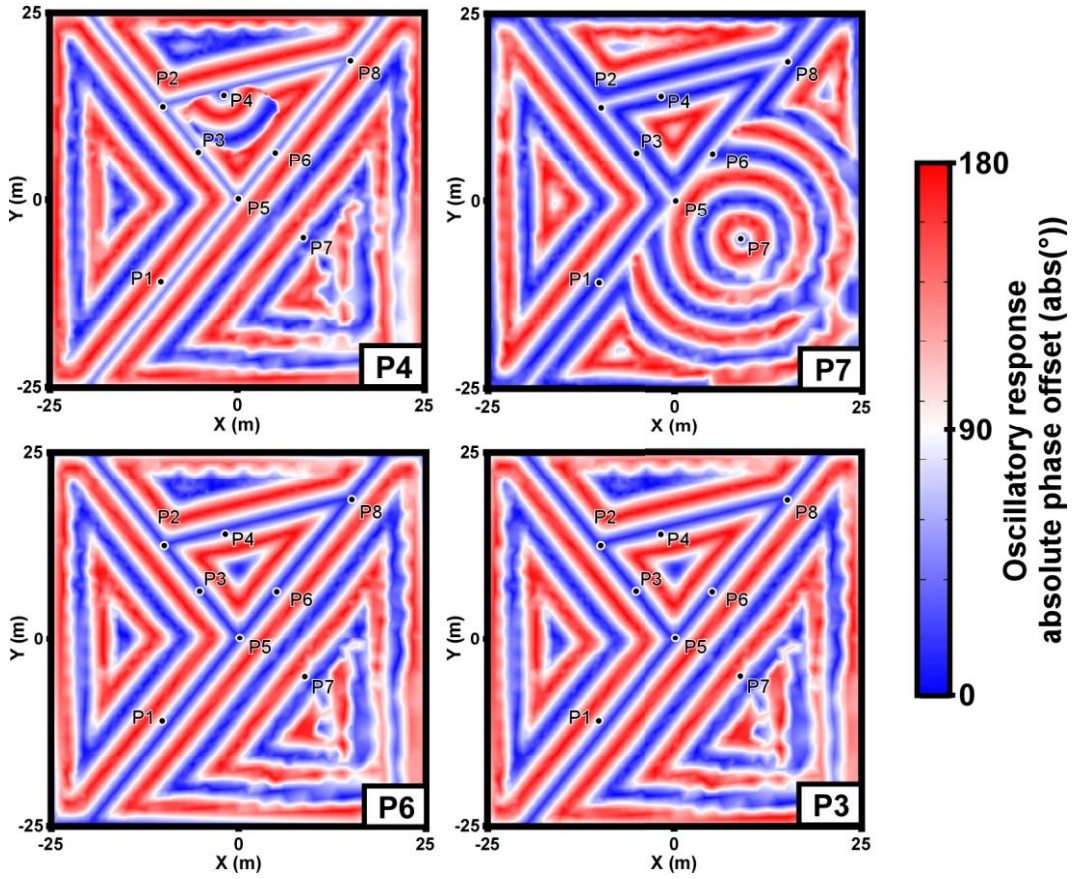

Figure 8: Maps of distribution of the phase offset value in the responses to a harmonic pumping signal with a 5 min period at different locations: in the matrix near a conduit (P4), in the matrix (P7), in a large conduit (P6), in a thin conduit (P3).

Concerning the spatial phase offset distribution in Figure 8, the case of a pumping in P7 in the matrix highlights what would be expected from a homogeneous aquifer. The phase offset value varies in function of the distance to the pumping point, forming a circle in the figure. As this circle reaches the network, its homogeneous behavior gets stopped, but at this position the signal has already lost its whole amplitude (see P7 in Figure 7). The same 'homogeneous behavior' can also be seen locally in the case of a pumping in P4 (in the matrix), but the phase offset variation gets quickly 'controlled' by the conduit's disposition. The phase offset remains then roughly constant along the network geometry, with a value dependent on the pumping point's distance to the network. For a direct pumping in the network (P6, P3), independently of the conduits conductivities (as long as these conductivities are significantly higher than the matrix), there is no significant phase shifting along the conduits of the network. For all cases,

403 once the signal has reached the karstic network, its phase shifting value will stay constant along
404 the conduits, but it will increase rapidly in flow paths orthogonal to the conduit (conduit to
405 matrix flows).

406 The effect of the signal period, already described in the previous part, can be generalized by
407 using these same maps (Figure 9).

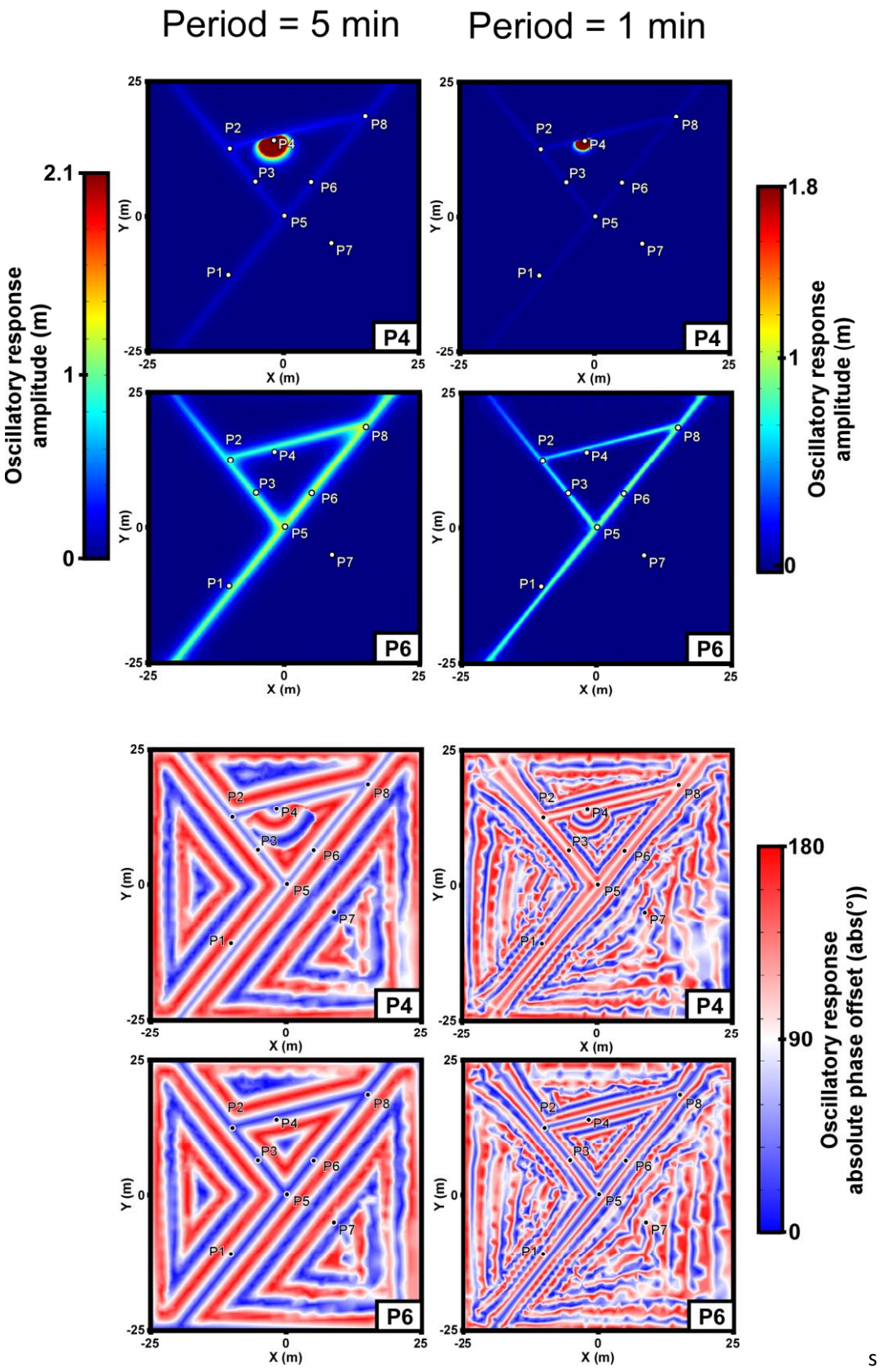

408 s

409 Figure 9: Comparative maps of distribution of the amplitude and absolute phase offset values
410 in the responses to a harmonic pumping at two different locations (in the matrix near a conduit
411 (P4), in a large conduit (P6)) for a 5 min period (left) and 1 min period (right) signal.

Figure 9 shows that a shorter period (high frequency) highlights more specifically the conduit network: the signal amplitude quickly decreases and the phase offset quickly increases when the signal enters the matrix. Thus, the propagation of the signal through diffusive flows in the matrix is almost absent. On the contrary a longer period signal can propagate at longer distances along matrix diffusive flows and with less phase shifting, which permits the boreholes in the matrix to respond. By comparing the cases of P6 in the figure, for a 5 min period the diffusive behavior of this signal seems to 'blur' the karstic network. In fact, the responses associated to boreholes located near the conduits become undistinguishable from the responses of boreholes located directly in the conduits, and thus a precise localization of the conduit will become more difficult. Concretely this behavior is seen for P1 or P4: their responses are close to the ones of in the conduits network for a 5 min period, but their responses for a 1 min period clearly show that they are located in the matrix.

4. Example of harmonic pumping investigation

4.1. Site presentation

We now apply the lessons learned from our analysis of synthetic data trends to a true field case. We have performed an oscillatory pumping test on the well-studied Terrieu karstic field (approximately 2,500 m²) near to Montpellier, in Southern France. The oscillations in the pumping rate were controlled by a programmable electrical device based on a dimmer, linked to the pump. This site has been studied in two recent thesis (Jazayeri Noushabadi 2009 ; Dausse 2015) and several articles (Jourde et al. 2002; Jazayeri Noushabadi et al. 2011; Wang et al. 2016 ; Wang et al. 2017). The property values used in the synthetic model are inspired from conduits, fractures, matrix and regional property estimations issued from investigations presented in Dausse (2015). The Terrieu karstic field is part of the MEDYCYSS observatory (Jourde et al.

2011), and an experimental site of the French National Karst Observatory (SNO Karst - *www.sokarst.org*).

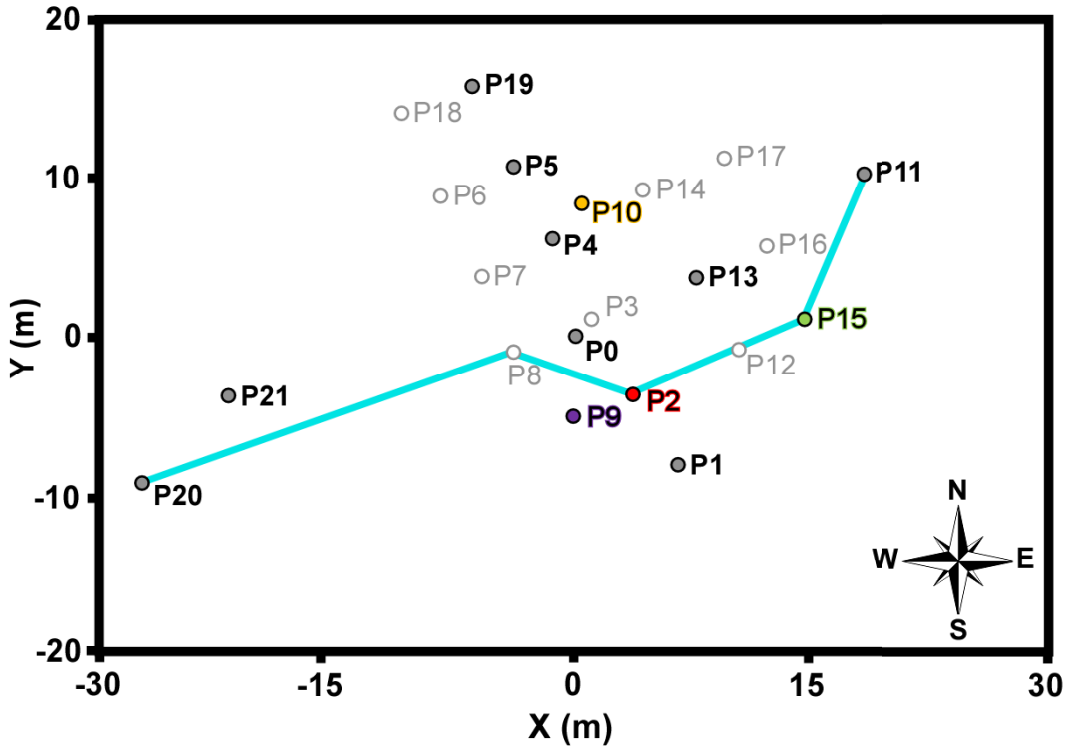

Figure 10: Boreholes locations on the Terrieu site. The colors for P2, P9, P10 and P15 refer to the colors used to designate these boreholes in Figure 11. The blue line indicates a conduit connectivity assessed from previous investigations (Dausse 2015; Wang et al. 2016). The boreholes in light grey were not measured during the harmonic pumping test.

This site is investigated through 22 boreholes (Figure 10) and lies on a confined aquifer. Observed conduits through downhole videos (Jazayeri Noushabadi et al. 2011), located between 35 m and 45 m under the surface, have been generated at a sloped and fractured interface between marly Cretaceous and massive Jurassic limestones. Both units have very low permeability, which permits to consider the karstic aquifer to be confined. At the time of the field investigation karst features located at the sloped interface were fully saturated. These conduits have an aperture that can reach 20 to 50 cm. Previous field investigations (packer tests, temperature and electrical conductivity logging) have permitted to highlight a preferential flow path (see blue line in Figure 10) within this karstified interface crossing several boreholes

453 (Jazayeri Noushabadi 2009; Dausse 2015). This preferential flow path could the consequence
454 of a network of conduits directly connecting these points.

455 A pumping investigation was conducted with an electronical automata device connected to the
456 pump and generating oscillations in the pumping rate. A harmonic pumping test was led for 30
457 min on the borehole P15 with a period of 5 min with flow rates that varied between 3.2 m^3/h
458 and 7.4 m^3/h. In other words, the signal from this pumping can be represented as a constant-
459 rate pumping test of magnitude 5.3 m^3/h (Q_m) convolved with an oscillatory (net zero) pumping
460 signal with period 5 minutes and amplitude 2.1 m^3/h (Q_A). The signal drawdown responses
461 were measured in 12 other boreholes, additionally to a measurement in the pumping borehole
462 itself.

463 ## 4.2. Example of typical responses

464 The upper graph in Figure 11 shows the drawdown measurement in the pumping borehole
465 (P15), and example of measured responses in three other boreholes (P2, P9 and P10). These
466 three boreholes are approximately at the same distance from the pumping point.

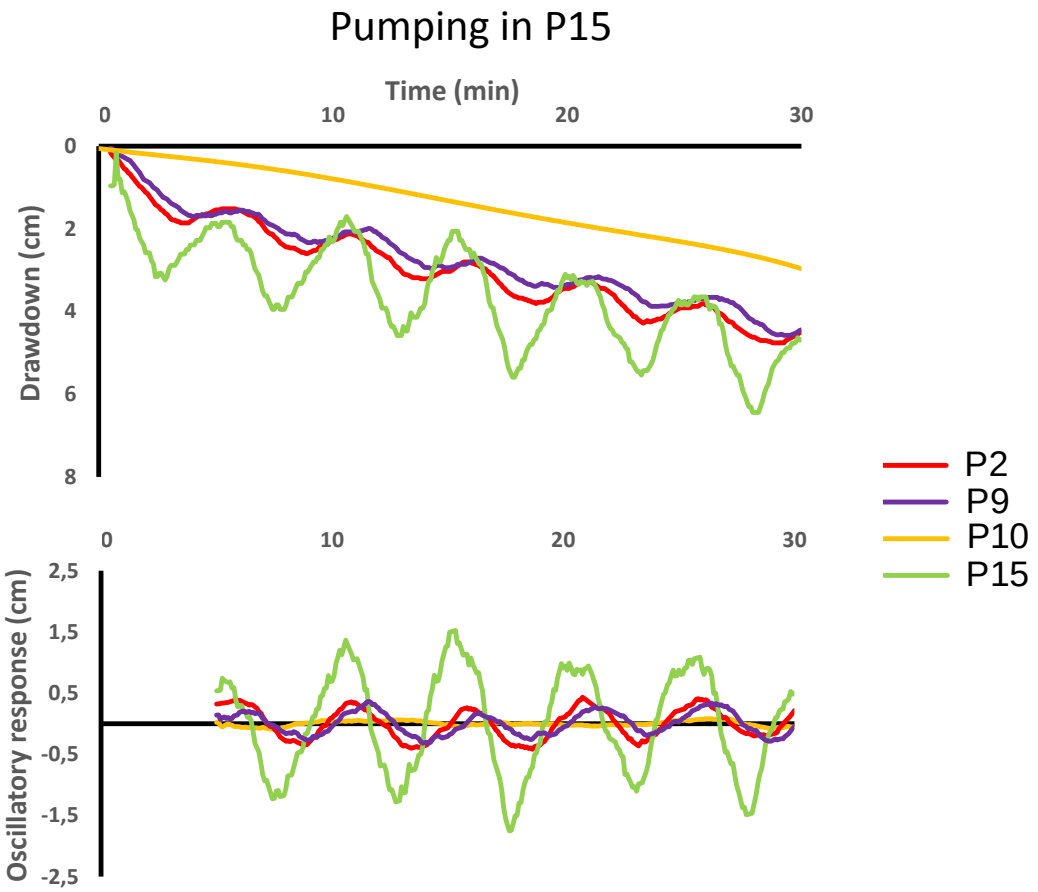

467

468 Figure 11: Example of different type of responses registered during the 5 min period harmonic
469 pumping test in P15 on the Terrieu site. The top graph shows the complete responses and the
470 bottom graph shows the purely oscillatory responses after having subtracted the linear signal.

471

472 This graph shows that the field measured responses have the same behavior as the theoretical
473 ones, with additional noise. The drawdown responses, if we pass over the first pumping period,
474 can be approximately decomposed as an addition of a purely linear signal and a purely
475 oscillatory signal of the form of Eq. 10 (shown in the lower graph of Figure 11). The amplitude
476 and phase offset analysis of the oscillatory signal of the three chosen measured responses
477 examples also show that we have the same type of responses in this field case as seen in the
478 theoretical case: responses with measurable amplitude and a low phase offset (P2), responses
479 with similar amplitude but a high phase offset (P9), and responses that contain no measurable

oscillatory component (P10). Therefore, it seems acceptable to test the same interpretation that we made on the theoretical case for the field data.

4.3. Interpretation of the responses

We decomposed the entire set of measured drawdowns (following Eq. 11) in order to keep only their oscillatory signal (the oscillatory responses in each borehole are presented in Figure 12). We have then fit these oscillatory signals to function of the form of Eq. 10 with amplitude and phase offset as variable parameters.

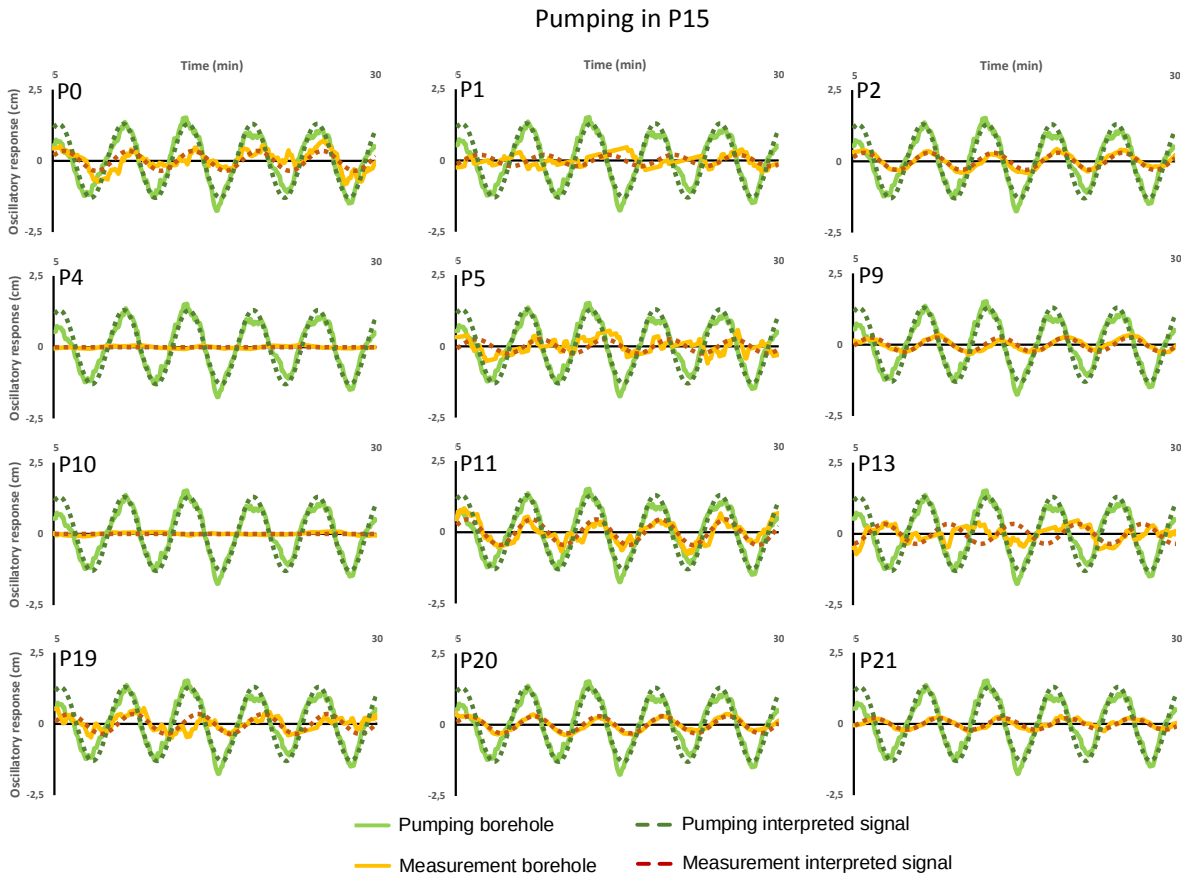

Figure 12: Registered oscillatory responses for each measurement borehole compared to the T= 5 min period pumping borehole signal (full lines) and the interpreted signals for an equation form of Eq. 10 with variables amplitude and phase offset values (dotted lines).

As for the interpretation of the amplitude and phase offset values from the frequency domain modeling of the theoretical case in Part 3.3.2, we have produced in Figure 13 a map of the measured amplitude and phase offset values from the oscillatory responses to pumping at a point within the karstic network.

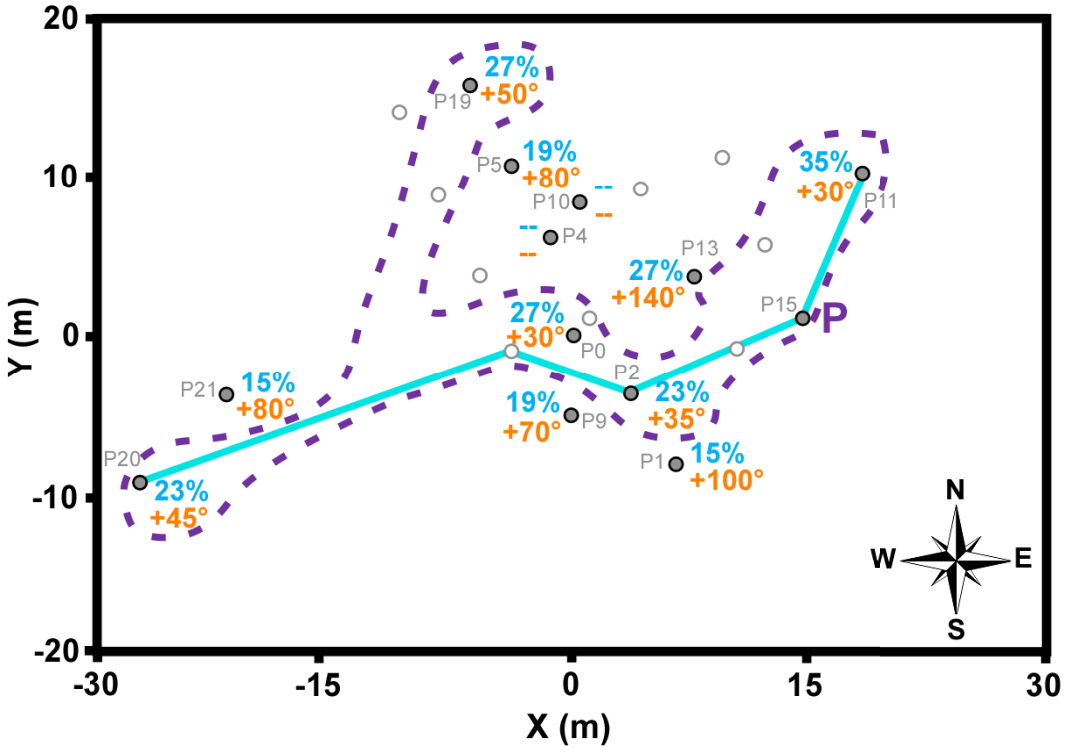

Figure 13: Example of a possible conduits network (inside the zone delineated by violet dotted boundaries) interpreted from the boreholes connectivity by applying the same analysis than in the synthetic case. The captions represent the relative amplitude (in blue, in %) and relative phase offset (in orange, in °) values in the oscillatory responses in each measured borehole. A dash represents an absence of oscillatory response (< 1 mm). The pumping location is indicated by 'P'. The blue line indicates a conduit connectivity known from previous investigations (Jazayeri Noushabadi 2009; Dausse 2015).

The relative amplitude values of the responses vary between 0% (no oscillatory response) and 35%, and the relative phase offset values vary between +30° and +140° (relatively to the pumping signal). From downhole observations and productivity estimations on the pumping well P15 (Jazayeri Noushabadi et al. 2011), we know that this well is located in a conduit of the network.

By analyzing the phase offset value, we note that the lower phase offset values are around +30°/+50°, and that several points have this same phase shift. This would indicate the presence of a network of conduits directly connecting these boreholes (‘conduit’ connectivity: P0, P2, P11, P19, P20) to the pumping point P15 (a possible network of conduits is proposed, within the zone delineated by the violet dotted boundaries, in Figure 13). Then, the other boreholes (‘dual’ connectivity: P1, P5, P9, P21; ‘matrix’ connectivity’: P4, P10) would have coherent responses toward this conduit network, similar to those seen in the study of the synthetic case (‘dual’ or ‘matrix’ connectivity). The more a borehole is distant to this possible conduit network, the more its response signal relatively to the pumping signal has a low amplitude and a high phase shift (for the more distant boreholes P4 and P10, the oscillatory signal disappear which indicate a ‘matrix’ connectivity). Only P13 would present an incoherent response (with both a high amplitude response and a high phase shift), but its true signal was too noisy to permit a good amplitude and phase offset parameters fitting (see P13 in Figure 12). This incoherent result can be attributed to a bad signal measurement. Except this point, the other 11 measured responses on the field are coherent with the behaviors interpreted in the theoretical study case.

The conduit connectivity highlighted from the method presented in this article is coherent with the direct connectivity already highlighted from previous investigations (blue line in Figure 13), which tend to strengthen the validity of this interpretation. Furthermore, P19, which was not found as connected in the previous investigation, appears to be directly connected in this work. However, this connectivity information would require a supplementary validation in the next field campaigns.

We have finally made quantitative estimation on the property values in the field, relatively to each response, in order to compare these estimations to the previously found degree of connectivity. These estimations were made by finding, for each response, an equivalent

535 homogeneous model (K_{eq} and $S_{S,eq}$) reproducing the response amplitude and phase offset. The
536 optimization of K_{eq} and $S_{S,eq}$ in each case was performed through a classical least square
537 minimization criterion inversion. It appears that P0, P2, P11, P20 (interpret as connected
538 through conduits), and P13 require high K_{eq} values (10^{-2} to 10 m/s) and low $S_{S,eq}$ (10^{-8} to 10^{-7}
539 m^{-1}). P5, P9, P21 (interpret as dual connectivity responses), and P19 (interpreted as directly
540 connected) require high K_{eq} values (10^{-3} to 10^{-2} m/s) and high $S_{S,eq}$ (10^{-4} to 10^{-3} m^{-1}). Finally,
541 P1 (interpreted as dual connectivity response), and P4 and P10 (interpreted as a prevailing
542 matrix connection) require low K_{eq} values (10^{-6} m/s) and high $S_{S,eq}$ (10^{-4} m^{-1}). Globally three
543 categories of estimated equivalent properties can also be highlighted and would correspond to
544 the previously described degree of connectivity: conduit connectivity (high K_{eq}, low $S_{S,eq}$),
545 dual connectivity (high K_{eq}, high $S_{S,eq}$), and matrix connectivity (low K_{eq}, high $S_{S,eq}$). In this
546 case only P19 appears to be rather connected in a ‘dual’ manner and P1 rather as a matrix point,
547 which nuance the interpretation of some responses at the limit of the defined categories.

548 From these results, we believe that the qualitative method of interpretation of harmonic signal
549 responses developed in this work can facilitate interpreting the degree of connectivity of karstic
550 field responses to an oscillatory signal, especially in order to characterize and localize the
551 conduits network through the boreholes connectivity. This interpretation can be led manually
552 as shown in this field example. However the next step would be to use this interpretation in an
553 inverse modeling approach (associated to a frequency domain modeling and by considering the
554 amplitude and phase offset values of the observed and simulated responses). This approach
555 becomes, in fact, very useful when the amount and complexity of responses to interpret is
556 important. The Cellular Automata-based Deterministic Inversion developed in Fischer et al.
557 (2017) would provide in this case interesting results, as it would permit to generate both
558 adequate conduits network and property distributions (conductivity and specific storage) for the

559 reproduction of the responses, and thus go further in the quantitative analysis of the harmonic
560 data in karstic fields.

561 5. Discussion and conclusion

562 We have studied the responses to harmonic pumping in a theoretical synthetic study, by
563 applying a time domain solver and a frequency domain solver. We have firstly demonstrated
564 that the harmonic result from the frequency domain simulation was very similar to the time
565 domain oscillatory part, and thus, as the frequency domain solver is much faster, it is more
566 useful for the simulation of periodic responses.

567 From an analysis of the amplitude and the phase offset of the response relative to the pumping
568 signal and its positioning in the model, we have proposed a global method for qualitatively
569 interpreting a degree of hydraulic connectivity between each borehole. The amplitude and phase
570 offset values permit to distinguish either a conduit connectivity between boreholes (flow path
571 in the conduit network), or a dual connectivity (flow path partly in the matrix for boreholes near
572 to a conduit but not directly in it), or a matrix connectivity (majority of flow associated with
573 flow in the matrix). By modifying the period of the pumping signal, we can dissociate more
574 precisely the conduit connectivity and the connectivity and obtain some information about the
575 distance of a measurement point relatively to the karstic network. A high frequency signal will
576 more specifically highlight the conduit flows, while a low frequency signal will give more
577 importance to the matrix diffusive flows.

578 In previous works Renner and Messar (2006) and Guiltinan and Becker (2015) used analytical
579 solutions to show that, in a fractured aquifer, increasing the pumping period decreased the
580 estimates of effective hydraulic diffusivity, due to the increase of the values of estimated
581 storativity (while the transmissivity estimations remained almost unchanged), which was
582 associated to a mobilization of the surrounding fracture void spaces. In our karstic model this

583 observation would be related to the behavior of a well in the matrix near to a conduit, where the
584 signal can better propagate within the high storage that represents the matrix when the pumping
585 period is increased. As it has been noticed by Rabinovich et al. (2015) with the use of a
586 heterogeneity model for a porous aquifer, flows (by extension the harmonic signal) will
587 preferentially propagate in the most conductive media, especially at lower pumping period,
588 which is also what we observe in our karstic model between conduits and matrix flows, when
589 pumping at different periods. The results we present in this article between amplitude ratio and
590 phase shifting and the degree of connectivity of boreholes show equivalent relations (in a more
591 accentuated way) than those presented by Guiltinan and Becker (2015) in a fractured aquifer.
592 The harmonic signal will arrive with an important attenuation and phase shift between areas
593 badly connected and, on the contrary, almost unchanged when fractures (or in our case a
594 conduit) connect two boreholes.

595 In order to test the validity of our signal analysis method, we have confronted the same
596 interpretation for a set of responses from a true karstic field to a harmonic pumping. The
597 interpretation permitted to delineate the main flow paths easily and quickly by satisfying all
598 measurement. This method could be generalized for a manual interpretation of a set of field
599 responses. The benefits brought here by the harmonic tests compared to the other connectivity
600 investigations done on the same site (packers, temperature and electrical conductivity) and to
601 constant-rate pumping can be found in the easier extraction of the signal in the responses (with
602 filtering techniques), even when responses are noised, and from the possibility to simulate the
603 responses with a modeling in a frequency domain, much quicker than the time domain.
604 Furthermore, the possibility of simulating the amplitude and phase offset values in the responses
605 using a frequency domain modeling permits a more affordable application of this interpretation
606 method in an inversion approach.

We have presented in the field part only the results from one pumping test associated to one period, selected from a campaign of pumping tests in which several different boreholes and different period values were tested. In order to interpret simultaneously all responses from all harmonic pumping tests, we have to use an inverse modeling. This technique is already widely used to characterize and quantify the heterogeneity in fractured and karstic fields, by interpreting the responses to constant-rate pumping hydraulic tomography (Hao et al. 2008 ; Illman et al. 2009 ; Castagna et al. 2011 ; Illman 2014 ; Zha et al. 2016 ; Wang et al. 2017). In a future work, we plan to focus more specifically our discussion on the quantitative analysis of the harmonic pumping responses in a karstic field, by associating them to a conduit network hydraulic imagery, based on an inverse modeling approach and its ability to reproduce the complete set of responses with a given distribution of properties.

Acknowledgments

We thank the region Normandy for financially supporting the PhD of Pierre Fischer. We would like to thank the four anonymous reviewers for their relevant comments and propositions which permitted to significantly improve the quality of this article.

Appendix

Appendix 1: Oscillatory response amplitude and phase offset values at the position of the different boreholes for a harmonic pumping in P3. We have estimated these values from a frequency domain simulation and from a time domain simulation (avoiding the first signal period). One sees that these values are almost the same for the two simulations.

	Frequency domain simulation		**Time domain simulation**	
	Amplitude (m)	**Phase offset (°)**	**Amplitude (m)**	**Phase offset (°)**
P1	0.4	70	0.4	72
P2	1.51	11	1.51	12
P3	2.1	8	2.1	9
P4	0.81	41	0.81	42
P5	1.15	14	1.15	15
P6	1.1	14	1.11	15
P7	0	--	--	--
P8	1.03	15	1.03	15

Appendix 2: Table of the real and relative amplitude and phase offset values in the oscillatory responses to different harmonic pumping locations and for two different signal periods. For each pumping case, the boreholes are sort by increasing distance to the pumping point. A dash represents an absence of oscillatory response (< 1 mm).

			Period = 5 min				**Period = 1 min**			
Pumping Point	**Borehole**	**Distance (m)**	**Amplitude (m)**	**Phase offset (°)**	**Relat. amplitude (%)**	**Relat. phase offset (°)**	**Amplitude (m)**	**Phase offset (°)**	**Relat. amplitude (%)**	**Relat. phase offset (°)**
P3	**P3**	0	2.1	8	100	0	1.81	11	100	0
	P2	8	1.51	11	72	3	1.23	16	68	5
	P5	8	1.15	14	54	6	0.89	21	49	10
	P4	8	0.81	41	39	33	0.34	84	19	73
	P6	10	1.1	14	53	6	0.85	22	47	11
	P1	18	0.4	70	19	62	0.1	149	6	138
	P7	18	--	--	--	--	--	--	--	--
	P8	24	1.03	15	49	7	0.78	23	43	12
P4	**P4**	0	236.31	9	100	0	191.12	20	100	0
	P2	8	0.26	39	0.11	30	0.11	80	0.06	60
	P3	8	0.2	41	0.09	33	0.09	84	0.05	64
	P6	10	0.15	45	0.06	36	0.06	90	0.03	69
	P5	14	0.15	45	0.06	36	0.06	90	0.03	70
	P8	18	0.16	44	0.07	35	0.16	88	0.08	68
	P7	22	--	--	--	--	--	--	--	--
	P1	26	0.05	101	0.02	92	0.06	-142	0.03	-162
P6	**P6**	0	1.38	12	100	0	1.12	17	100	0
	P5	8	1.3	12	94	1	1.04	18	93	1
	P3	10	1.1	14	80	3	0.85	22	76	5
	P4	10	0.61	45	44	33	0.25	90	22	73
	P7	12	--	--	--	--	--	--	--	--
	P8	16	1.23	13	89	1	0.97	19	87	2
	P2	16	0.93	17	67	5	0.69	25	62	9
	P1	23	0.46	68	33	57	0.12	146	11	129
P7	**P7**	0	174.03	22	100	0	110.86	40	100	0
	P5	10	--	--	--	--	--	--	--	--
	P6	12	--	--	--	--	--	--	--	--
	P3	18	--	--	--	--	--	--	--	--
	P1	20	--	--	--	--	--	--	--	--
	P4	22	--	--	--	--	--	--	--	--
	P8	24	--	--	--	--	--	--	--	--
	P2	26	--	--	--	--	--	--	--	--

633 # References

634 Bakhos, T., M. Cardiff, W. Barrash, P.K. Kitanidis. 2014. Data processing for oscillatory
635 pumping tests. *Journal of Hydrology* 511: 310-319.

636

637 Black, J.H., and K.L. Kipp Jr. 1981. Determination of hydrogeological parameters using
638 sinusoidal pressure tests: A theoretical appraisal. *Water Resources Research* 17 (No. 3): 686-
639 692.

640

641 Butler, J.J. 2005. Hydrogeological methods for estimation of spatial variations in hydraulic
642 conductivity. In: Rubin, Y., S.S. Hubbard. Hydrogeophysics. *Water Science and Technology*
643 *Library* (vol. 50). Springer, Dordrecht.

644

645 Cardiff, M., W. Barrash, P.K. Kitanidis, B. Malama, A. Revil, S. Straface, E. Rizzo. 2009. A
646 potential-based inversion of unconfined steady-state hydraulic tomography. *Ground Water* 47:
647 259–270.

648

649 Cardiff, M., T. Bakhos, P.K. Kitanidis, W. Barrash. 2013. Aquifer heterogeneity
650 characterization with oscillatory pumping: Sensitivity analysis and imaging potential. *Water*
651 *Resources Research* 49: 5395-5410.

652

653 Cardiff, M. and W. Barrash. 2015. Analytical and semi-analytical tools for the design of
654 oscillatory pumping tests. *Groundwater* 53 (No. 6): 896-907.

Castagna, M., M.W. Becker, A. Bellin. 2011. Joint estimation of transmissivity and storativity in a bedrock fracture. *Water Resources Research* 47: W09504 doi: 10.1029/2010WR009262.

Dagan, G., and A. Rabinovich. 2014. Oscillatory pumping wells in phreatic, compressible, and homogeneous aquifers. *Water Resources Research* 50 (No.8): 7058-7066.

Dausse, A. 2015. Facteurs d'échelle dans la hiérarchisation des écoulements au sein d'un aquifère karstique: Analyse multi-échelles des propriétés hydrodynamiques et de transport de l'aquifère du Lez. PhD Thesis, Université de Montpellier. French.

Fischer, P., A. Jardani, N. Lecoq. 2017. A cellular automata-based deterministic inversion algorithm for the characterization of linear structural heterogeneities. *Water Resources Research* 53: 2016-2034.

Guiltinan, E., and M.W. Becker. 2015. Measuring well hydraulic connectivity in fractured bedrock using periodic slug tests. *Journal of Hydrology* 521: 100-107.

Hao, Y., T.C.J. Yeh, J. Xiang, W.A. Illman, K. Ando, K.C. Hsu, C.H. Lee. 2008. Hydraulic tomography for detecting fracture zone connectivity. *Ground Water* 46: 183-192.

676 Illman, W.A. 2014. Hydraulic tomography offers improved imaging of heterogeneity in
677 fractured rocks. *Groundwater* 52: 659-684.

678

679 Illman, W.A., X. Liu, S. Takeuchi, T.C.J. Yeh, K. Ando, H. Saegusa. 2009. Hydraulic
680 tomography in fractured granite: Mizunami underground research site, Japan. *Water Resources*
681 *Research* 45: W01406 doi: 10.1029/2007WR006715.

682

683 Jazayeri Noushabadi, M.R. 2009. Characterization of relationship between fracture network
684 and flow-path network in fractured and karstic reservoirs: Numerical modeling and field
685 investigation (Lez aquifer, Southern France). PhD Thesis, Université de Montpellier. English.

686

687 Jazayeri Noushabadi, M.R., H. Jourde, G. Massonnat. 2011. Influence of the observation scale
688 on permeability estimation at local and regional scales through well tests in a fractured and
689 karstic aquifer (Lez aquifer, Southern France). *Journal of Hydrology* 403: 321-336.

690

691 Jourde, H., F. Cornaton, S. Pistre, P. Bidaux. 2002. Flow behavior in a dual fracture network.
692 *Journal of hydrology* 266: 99-119.

693

694 Jourde, H., C. Batiot-Guilhe, V. Bailly-Comte, C. Bicalho, M. Blanc, V. Borrell, C. Bouvier,
695 J.F. Boyer, P. Brunet, M. Cousteau, C. Dieulin, E. Gayrard, V. Guinot, F. Hernandez, L. Kong-
696 A-Siou, A. Johannet, V. Leonardi, N. Mazzilli, P. Marchand, N. Patris, S. Pistre, J.L. Seidel,
697 J.D. Taupin, and S. Van-Exter. 2011. The MEDYCYSS observatory, a multi scale observatory

698 of flood dynamics and hydrodynamics in karst (Mediterranean border Southern France). In:
699 Lambrakis, N., G. Stournaras, K. Katsanou. Advances in the research of aquatic environment.
700 *Environmental Earth Sciences*. Springer, Berlin, Heidelberg.

701

702 Lavenue, M., G. de Marsily. 2001. Three-dimensional interference test interpretation in a
703 fractured aquifer using the pilot point inverse method. *Water Resources Research* 37 (No. 11):
704 2659-2675.

705

706 Liedl, R., M. Sauter, D. Huckinghaus, T. Clemens, G. Teutsch. 2003. Simulation of the
707 development of karst aquifers using a coupled continuum pipe flow model. *Water Resources*
708 *Research* 39, 1057.

709

710 Maineult, A., E. Strobach, J. Renner. 2008. Self-potential signals induced by periodic pumping
711 tests. *Journal of Geophysical Research* 113: B01203 doi: 10.1029/2007JB005193.

712

713 Rabinovich, A., W. Barrash, M. Cardiff, D.L. Hochstetler, T. Bakhos, G. Dagan, P.K. Kitanidis.
714 2015. Frequency dependent hydraulic properties estimated from oscillatory pumping tests in an
715 unconfined aquifer. *Journal of Hydrology* 531: 2-16.

716

717 Rasmussen, T.C., K.G. Haborak, M.H. Young. 2003. Estimating aquifer hydraulic properties
718 using sinusoidal pumping at the Savannah River site, South California, USA. *Hydrogeology*
719 *Journal* 11: 466-482.

Renard, P., and D. Allard. 2013. Connectivity metrics for subsurface flow and transport. *Advances in Water Resources* 51: 168-196.

Renner, J., M. Messar. 2006. Periodic pumping tests. *Geophysical Journal International* 167: 479-493.

Saller, A.P., M.J. Ronayne, A.J. Long. 2013. Comparison of a karst groundwater model with and without discrete conduit flow. *Hydrogeology Journal* 21: 1555-1566.

Schuite, J., L. Longuevergne, O. Bour, N. Guihéneuf, M.W. Becker, M. Cole, T.J. Burbey, N. Lavenant, F. Boudin. 2017. Combining periodic hydraulic tests and surface tilt measurements to explore in situ fracture hydromechanics. *Journal of Geophysical Research: Solid Earth* 122: 6046-6066.

Soueid Ahmed, A., A. Jardani, A. Revil, J.P. Dupont. 2016. Joint inversion of hydraulic head and self-potential data associated with harmonic pumping tests. *Water Resources Research* 52 (No. 9): 6769-6791.

Sun, A. Y., J. Lu, and S. Hovorka. 2015. A harmonic pulse testing method for leakage detection in deep subsurface storage formations. *Water Resources Research* 51: 4263–4281.

742 Sun, A. Y., J. Lu, B. M. Freifeld, S. D. Hovorka, and A. Islam. 2016. Using pulse testing for
743 leakage detection in carbon storage reservoirs: A field demonstration. *International Journal of*
744 *Greenhouse Gas Control* 46: 215-227.

745

746 Teutsch, G. 1993. An extended double-porosity concept as a practical modeling approach for a
747 karstified terrain. *Hydrogeological Processes in Karst Terranes* 207: 281-292.

748

749 Tyukhova, A. R., and M. Willmann. 2016. Connectivity metrics based on the path of smallest
750 resistance. *Advances in Water Resources* 88: 14-20.

751

752 Wang, X., A. Jardani, H. Jourde, L. Lonergan, J. Cosgrove, O. Gosselin, and G. Massonat.
753 2016. Characterisation of the transmissivity field of a fractured and karstic aquifer, Southern
754 France. *Advances in Water Resources* 87: 106-121.

755

756 Wang, X., A. Jardani, and H. Jourde. 2017. A hybrid inverse method for hydraulic tomography
757 in fractured and karstic media. *Journal of Hydrology* 551: 29-46.

758

759 White, W.B. 2002. Karst hydrology: recent developments and open questions. *Engineering*
760 *Geology* 65: 85-105.

761

762 Zha, Y., T.C.J. Yeh, W.A. Illman, T. Tanaka, P. Bruines, H. Onoe, H. Saegusa, D. Mao, S.
763 Takeuchi, J.-C. Wen. 2016. An application of hydraulic tomography to a large-scale fractured
764 granite site, Mizunami, Japan. Groundwater 54: 793-804.

765

766 Zhou, Y., D. Lim, F. Cupola, M. Cardiff. 2016. Aquifer imaging with pressure waves -
767 Evaluation of low-impact characterization through sandbox experiments. *Water Resources*
768 *Research* 52: 2141-2156.